

Supporting Information

For

In Situ Observations of the Occlusion of a Clay-Sugar Compound within Calcite

Jialin Chi,¹ Chonghao Jia,¹ Wenjun Zhang,¹ Christine V. Putnis,^{2,3} and Lijun Wang^{*,1}

¹College of Resources and Environment, Huazhong Agricultural University, Wuhan 430070,
China

²Institut für Mineralogie, University of Münster, 48149 Münster, Germany

³School of Molecular and Life Sciences, Curtin University, 6845 Perth, Australia

SI Tables (1-2)

SI Figures (1-14)

SI References

Table S1. Supersaturated solutions for calcite growth.

| σ | Concentration (mM) | | | pH |
|----------|--------------------|--|------|-----|
| | CaCl ₂ | K ₂ C ₂ O ₄ | NaCl | |
| 0.274 | 0.18 | 5.50 | 100 | 8.3 |
| 1.196 | 0.30 | 9.00 | 100 | 8.3 |

Table S2. Raman shifts (cm⁻¹) of laponite, glucose, dextran, and calcite.

| Composition | Wavenumber (cm ⁻¹) | Assignments |
|------------------------|--------------------------------|--|
| Laponite ¹ | 358, 683 | [SiO ₄] lattice mode |
| | 404 | CC bending |
| Glucose ² | 424 | CCC bending |
| | 521 | CCO bending |
| | 407 | CC bending |
| Dextran ^{2,3} | 441 | CCO endocyclic bending |
| | 540 | CCO bending |
| Calcite ⁴ | 713 | CO ₃ ²⁻ in-plane bending |
| | 1086 | CO symmetric stretching |

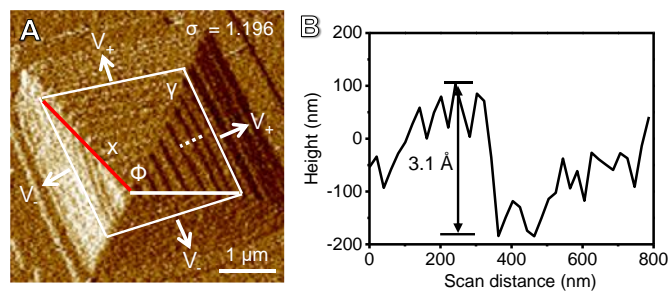


Figure S1. (A) AFM deflection images of the $(10\bar{1}4)$ cleavage surface of calcite, showing a rhombohedral growth spiral with (B) height of 3.1 \AA along a white dashed line in (A) in a solution supersaturated with respect to calcite at $\sigma = 1.196$ (pH 8.3 and $IS = 0.11 \text{ M}$).

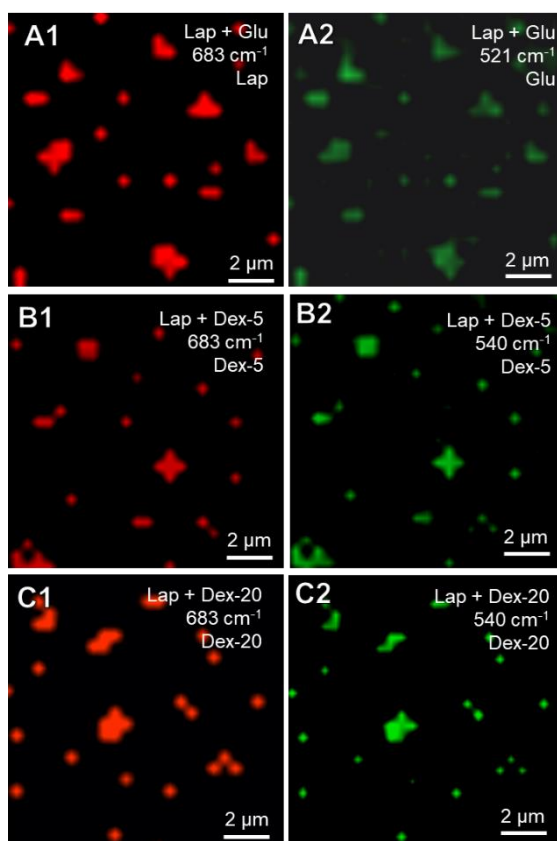


Figure S2. Raman mapping of 5 mg/L laponite at 683 cm^{-1} mixed with 2.5 mg/L sugars before elution at 521 or 540 cm^{-1} including (A) Glu, (B) Dex-5 and (C) Dex-20 deposited on tinfoil.

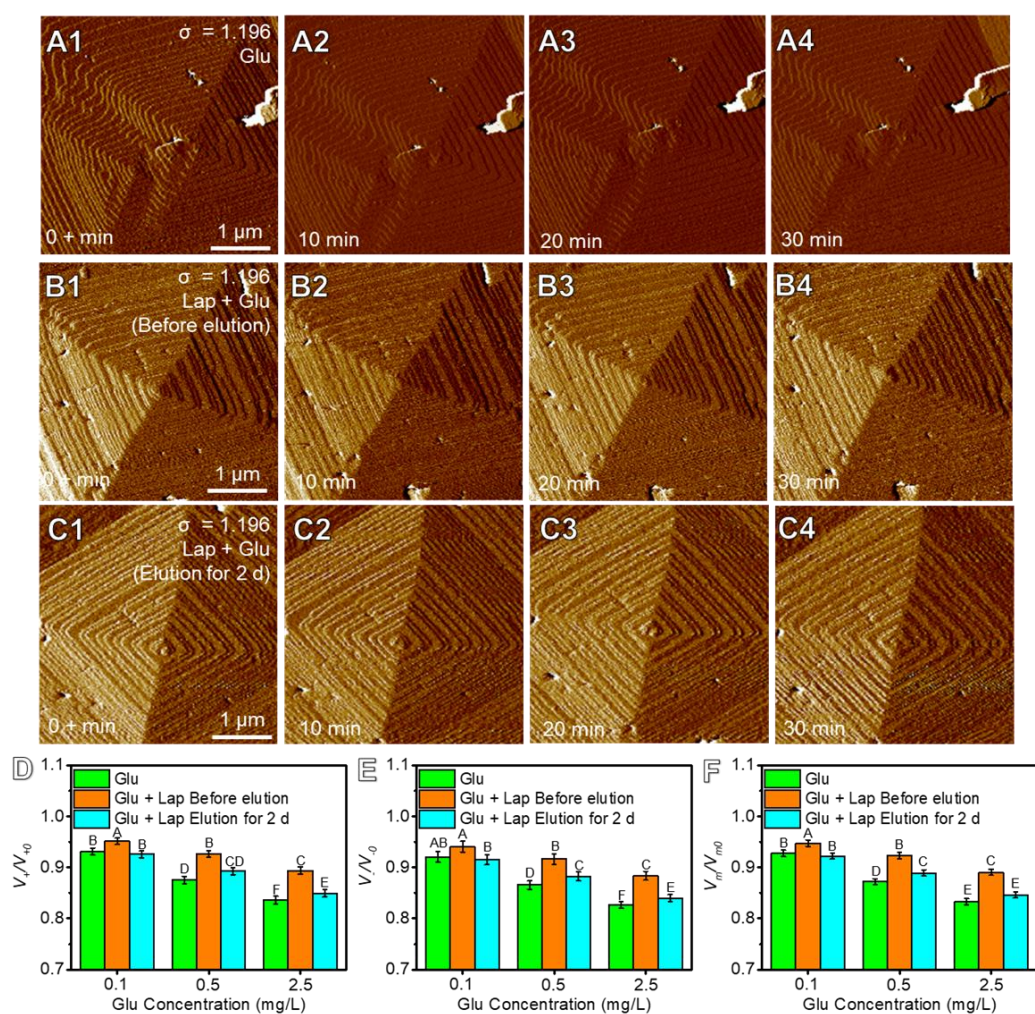


Figure S3. (A-C) AFM deflection images of growing hillocks (spirals) in a solution supersaturated with respect to calcite at $\sigma = 1.196$ and pH 8.3 in the presence of (A1-A4) Glu, (B1-B4) Glu + Lap complexes before elution, and (C1-C4) Glu + Lap complexes eluted for 2 d. (D-F) Relative step movement velocities of the (D) v_+ , (E) v_- and (F) sum of v_+ and v_- ($v_m = v_+ + v_-$) as a function of Glu concentrations in the presence of 5 mg/L laponite + Glu complexes before and after elution at $\sigma = 1.196$ (pH = 8.3).

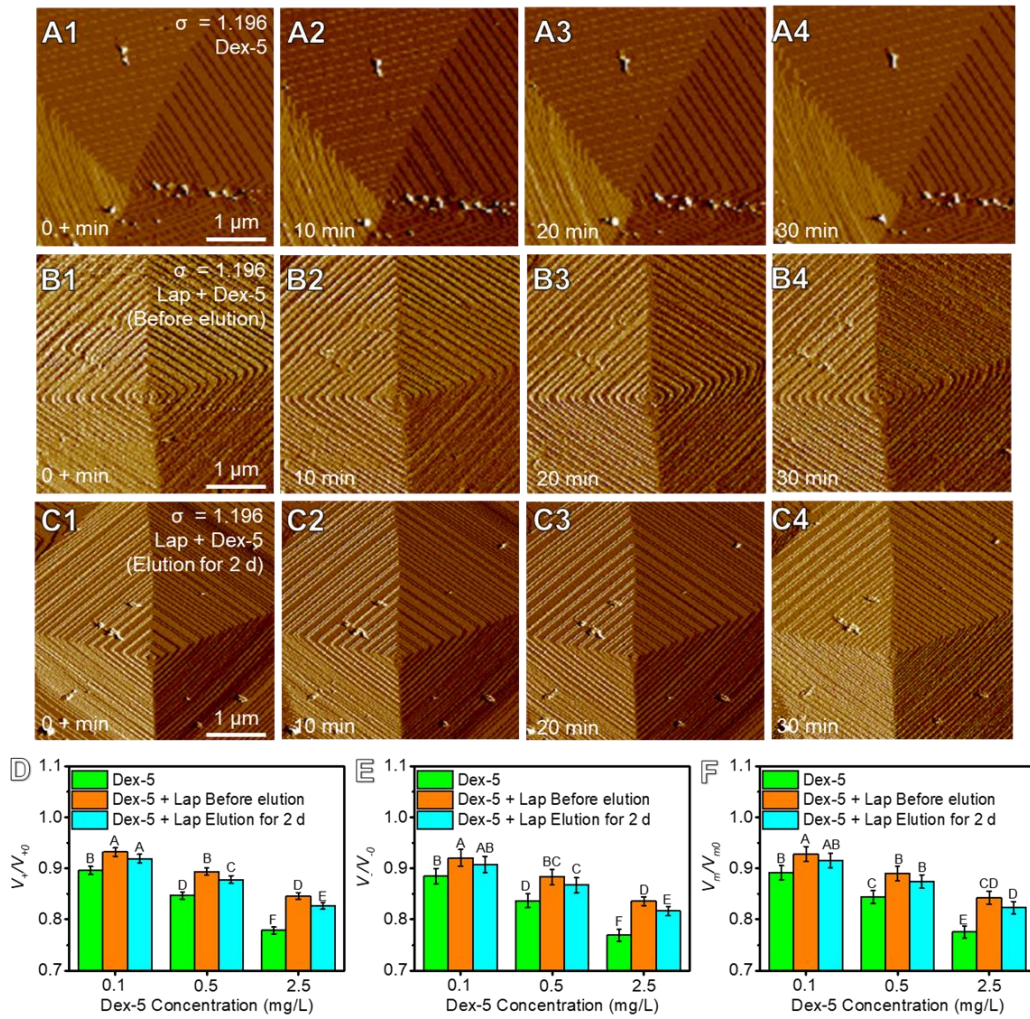


Figure S4. (A-C) AFM deflection images of growing hillocks (spirals) in a solution supersaturated with respect to calcite at $\sigma = 1.196$ and pH 8.3 in the presence of (A1-A4) Dex-5, (B1-B4) Dex-5 + Lap complexes before elution, and (C1-C4) Dex-5 + Lap complexes eluted for 2 d. (D-F) Relative step movement velocities of the (D) v_+ , (E) v_- and (F) sum of v_+ and v_- ($v_m = v_+ + v_-$) as a function of Dex-5 concentrations in the presence of 5 mg/L laponite + Dex-5 complexes before and after elution at $\sigma = 1.196$ (pH = 8.3).

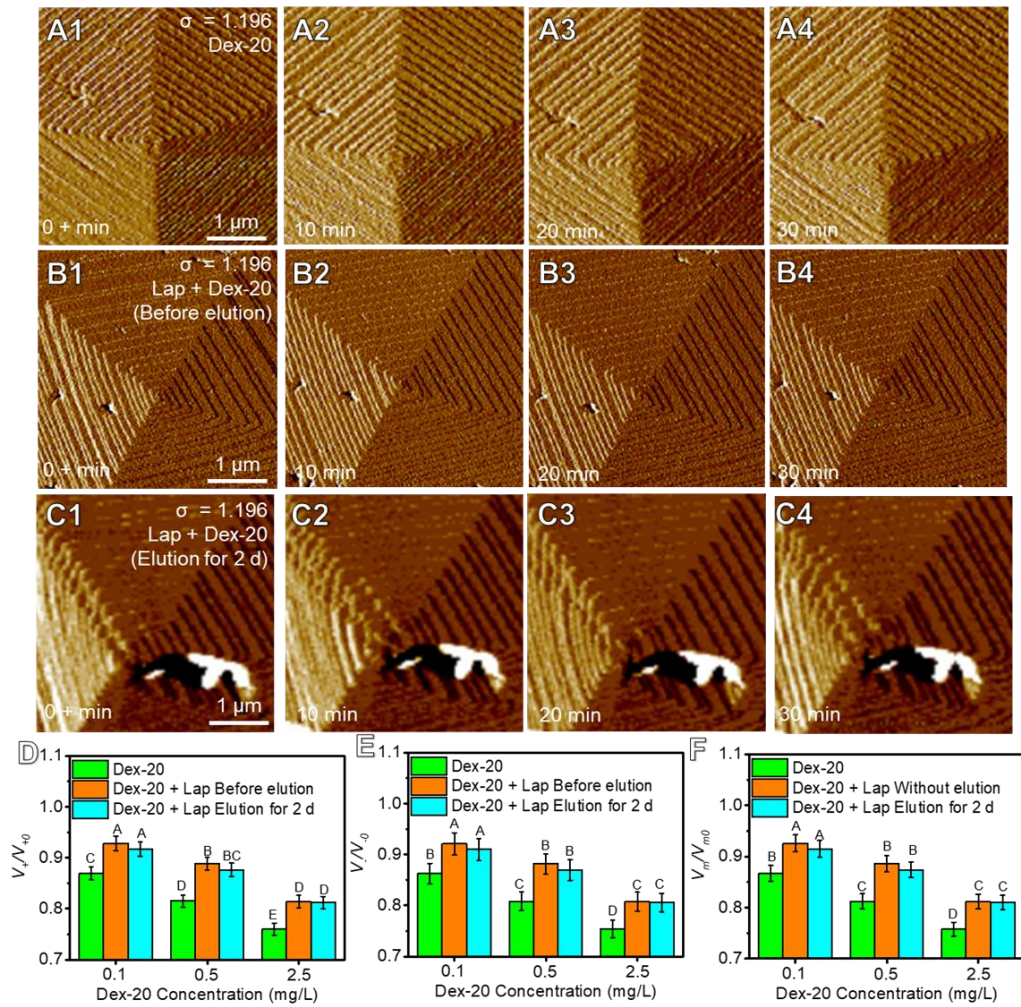


Figure S5. (A-C) AFM deflection images of growing hillocks (spirals) in a solution supersaturated with respect to calcite at $\sigma = 1.196$ and pH 8.3 in the presence of (A1-A4) Dex-20, (B1-B4) Dex-20 + Lap complexes before elution, and (C1-C4) Dex-20 + Lap complexes eluted for 2 d. (D-F) Relative step movement velocities of the (D) v_+ , (E) v_- and (F) sum of v_+ and v_- ($v_m = v_+ + v_-$) as a function of Dex-20 concentrations in the presence of 5 mg/L laponite + Dex-20 complexes before and after elution at $\sigma = 1.196$ (pH = 8.3).

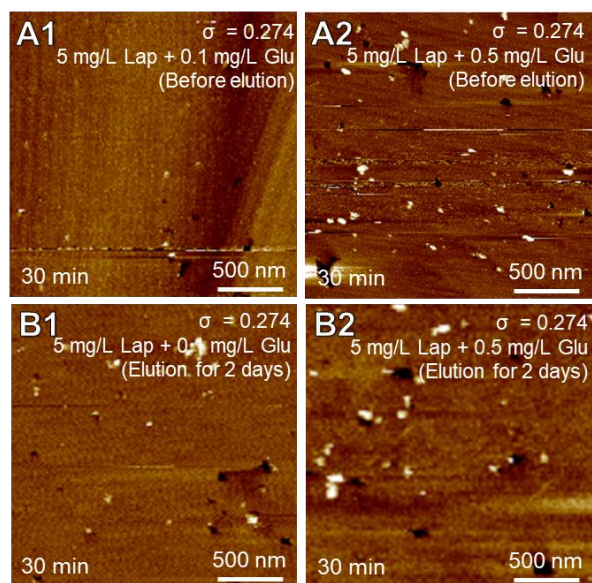


Figure S6. AFM height images of the adsorption of 5 mg/L laponite + Glu complexes (A1, A2) before and (B1, B2) after elution on calcite for 30 min with varied concentrations of Glu ($\sigma = 0.274$, pH = 8.3).

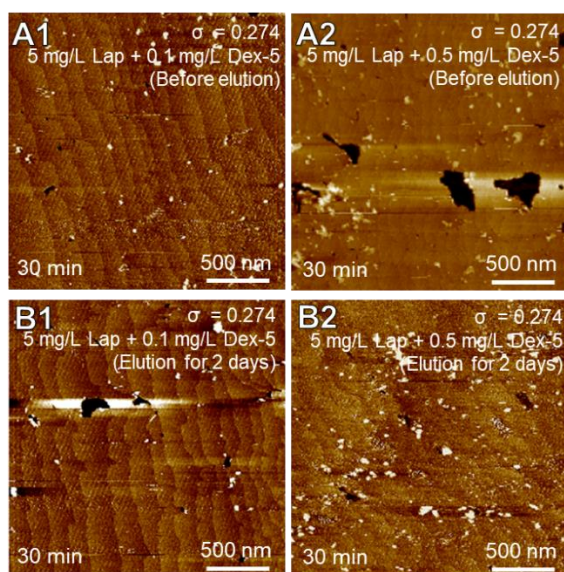


Figure S7. AFM height images of the adsorption of 5 mg/L laponite + Dex-5 complexes (A1, A2) before and (B1, B2) after elution on calcite for 30 min with varied concentrations of Dex-5 ($\sigma = 0.274$, pH = 8.3).

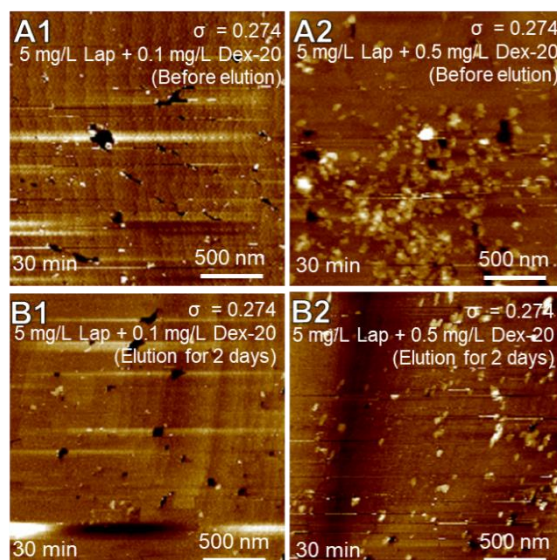


Figure S8. AFM height images of the adsorption of 5 mg/L laponite + Dex-20 complexes (A1, A2) before and (B1, B2) after elution on calcite for 30 min with varied concentrations of Dex-20 ($\sigma = 0.274$, pH = 8.3).

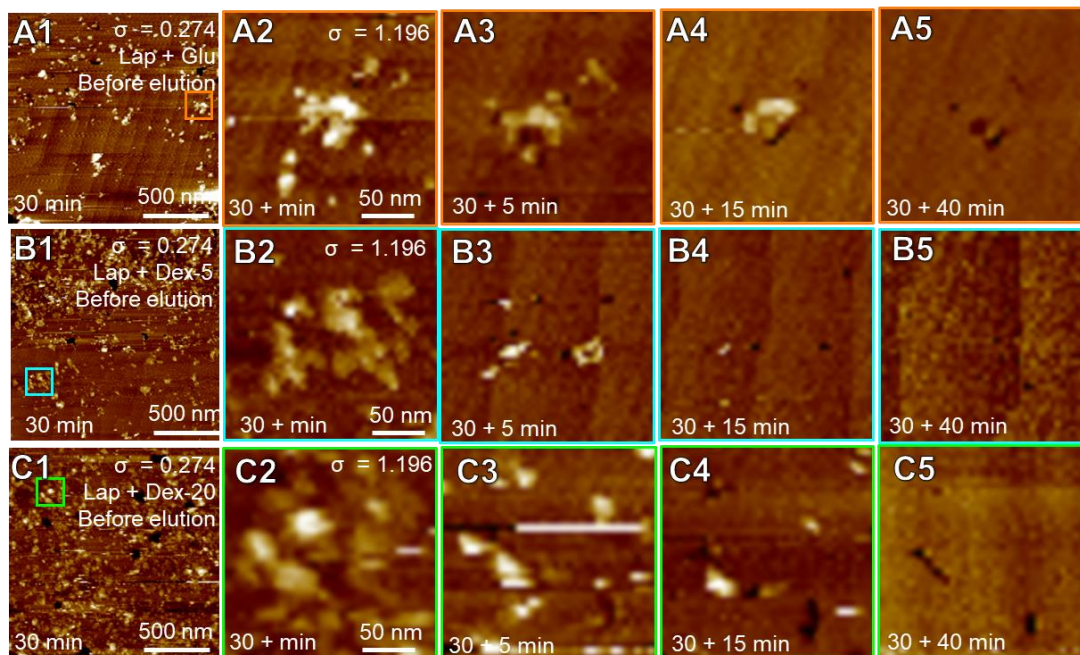


Figure S9. Time sequence of AFM height images of the adsorption and subsequent occlusion of laponite and sugar complexes before elution with concentrations of (A1-A4) 5 mg/L laponite + 2.5 mg/L Glu, (B1-B4) 5 mg/L laponite + 2.5 mg/L Dex-5, and (C1-C4) 5 mg/L laponite + 2.5 mg/L Dex-20 on a growing calcite surface.

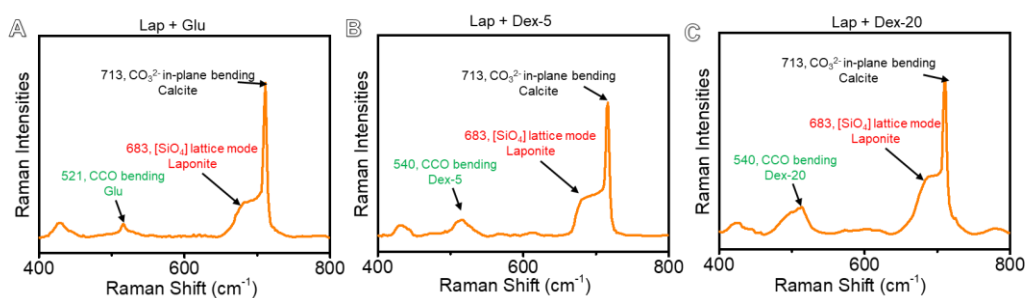


Figure S10. Raman spectra of adsorption and occlusion of sugar/laponite complexes (before elution) within calcite. The signals of calcite, laponite, and sugar are marked by arrows.

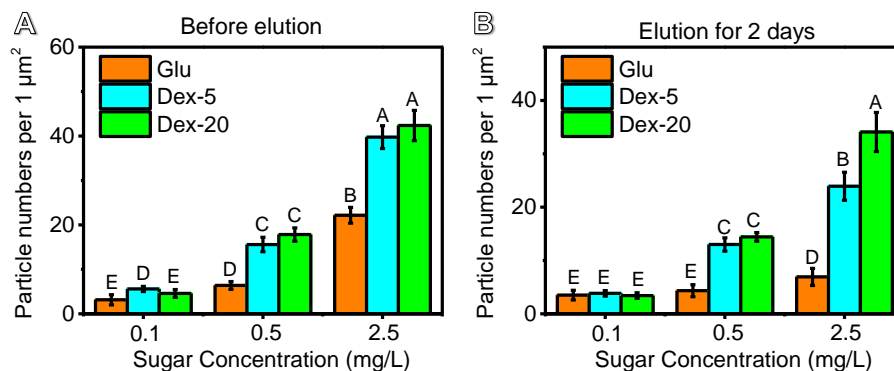


Figure S11. Particle number of 5 mg/L laponite + sugar complexes (A) before and (B) after elution with different concentrations of sugars adsorbed on a calcite surface prior to the occlusion process in an area of $1 \mu\text{m}^2$. Different uppercase letters in (A, B) indicate significant differences at $P < 0.01$.

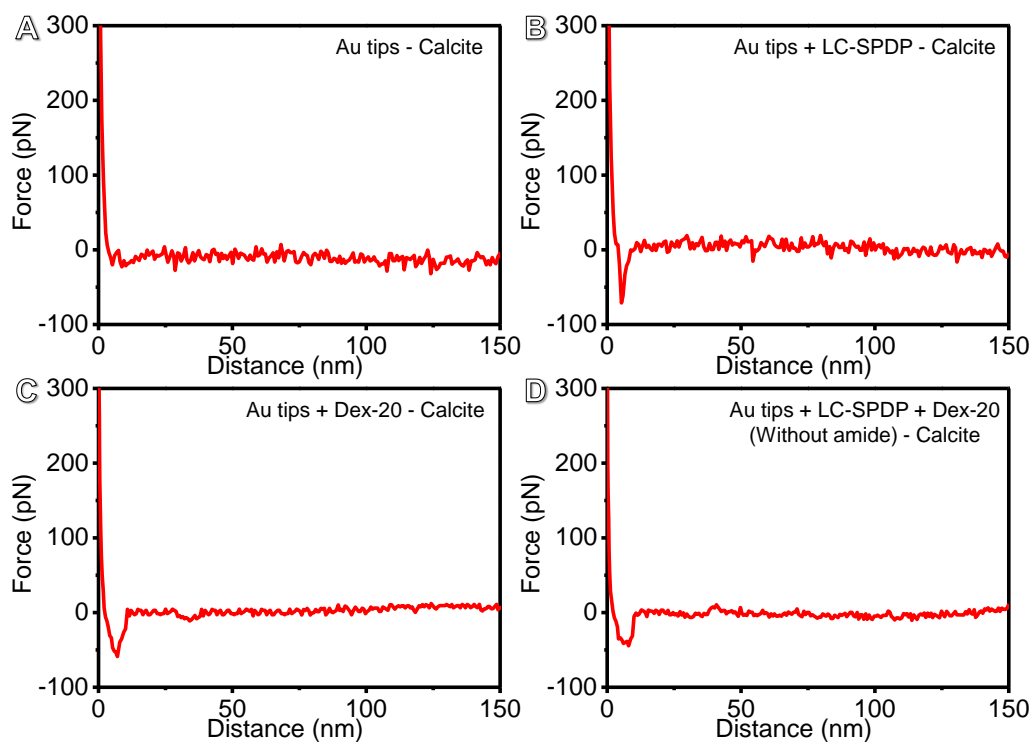


Figure S12. Representative force-distance curves of the interactions between (A) bare Au-coated tips, (B) Au-coated tips modified with LC-SPDP, (C) Au-coated tips + Dex-20, and (D) Au-coated tips + LC-SPDP + Dex-20 (Without amide) on calcite.

immersed in amide-modified Dex-20 for 12 h, and (D) Au-coated tips modified with LC-SPDP immersed in Dex-20 for 12 h, and calcite surfaces.

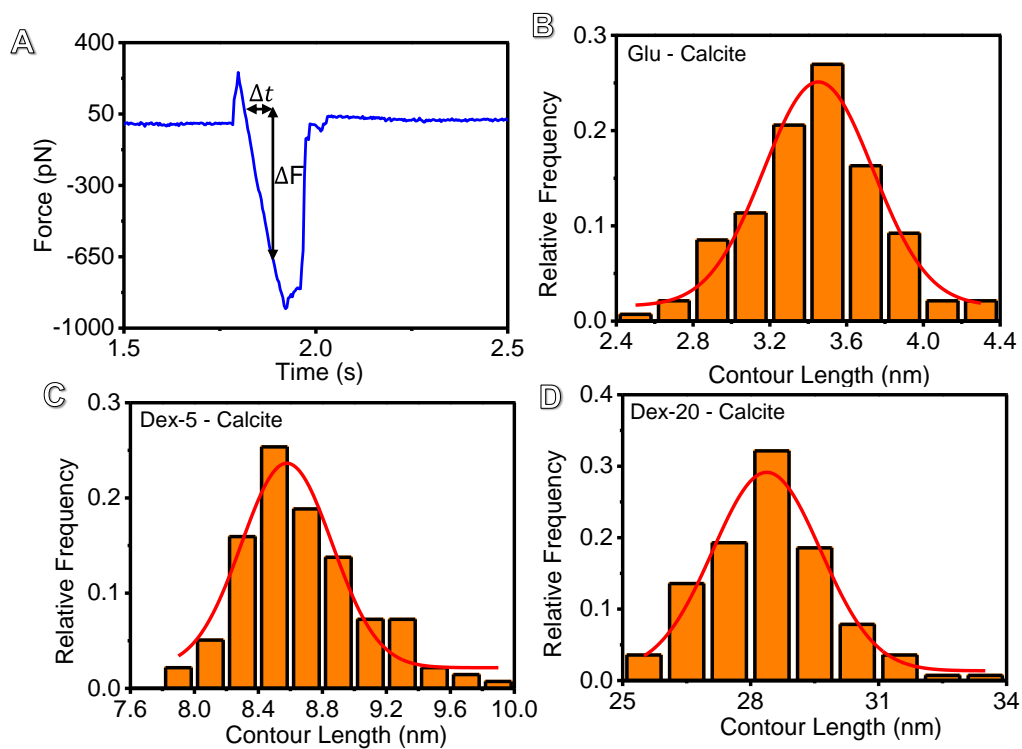


Figure S13. (A) A representative force–time curve of the interactions between amide-modified Dex-20 and a calcite surface. (B-D) The fitted contour length for different amide-modified sugars (including Glu, Dex-5, and Dex-20) with calcite surfaces.

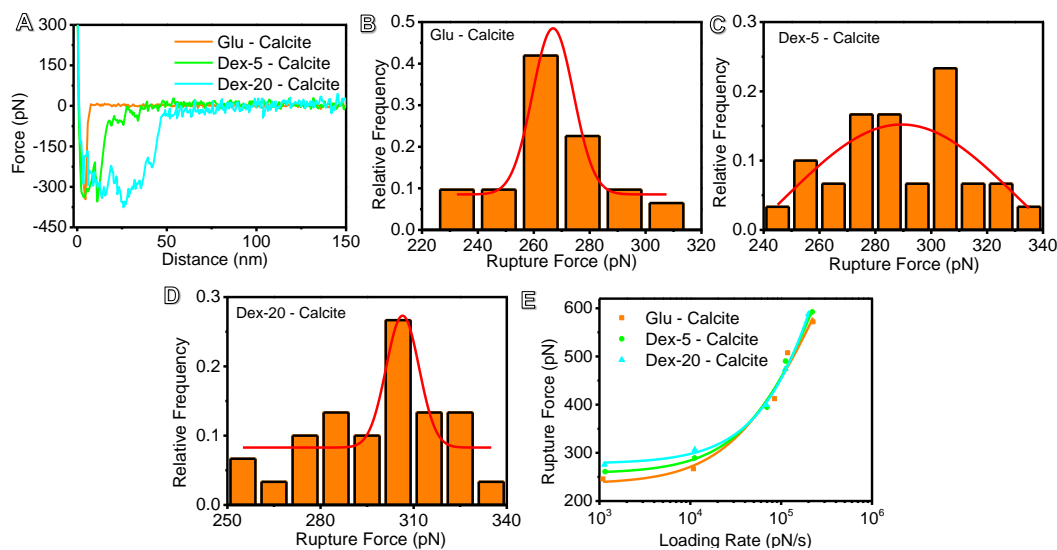


Figure S14. (A) Representative force-distance curves of the interactions between amide-modified sugars and calcite surfaces. (B-D) The rupture forces between amide-modified sugars and calcite surfaces at a loading rate of 200 nm/s. (E) The fitted rupture force curves of various amide-modified sugars interacting with calcite surfaces.

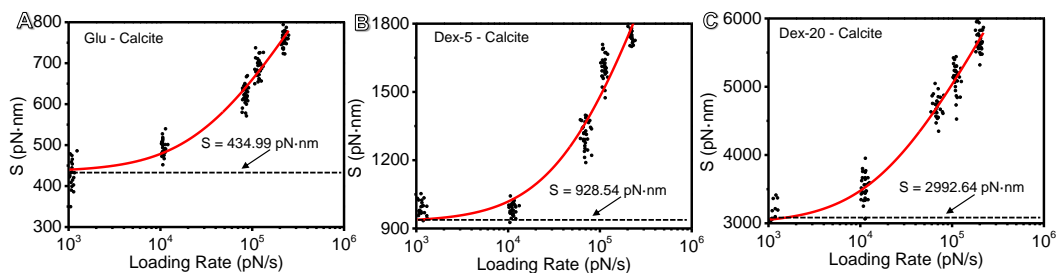


Figure S15. The fitted total force during stretching force or interaction area curves of amide-modified sugars interacted with calcite surfaces.

SI References

- (1) G. F. Perotti, J. Tronto, M. A. Bizeto, C. M. S. Izumi, M. L. A. Temperini, A. B.

Lugão, D. F. Parra and V. R. L. Constantino, Biopolymer-clay nanocomposites: Cassava starch and synthetic clay cast films, *Braz. Chem. Soc.*, 2014, **25**, 320-330.

(2) M. Mathlouthi, Laser-Raman spectra of d-glucose and sucrose in aqueous solution. *Carbohydr. Res.*, 1980, **81**, 203-212.

(3) M. Larsson, J. Lindgren, A. Ljunglöf, K. G. Knuuttila, Ligand distributions in agarose particles as determined by confocal Raman spectroscopy and confocal scanning laser microscopy, *Appl. Spectrosc.*, 2003, **57**, 251-255.

(4) L. Borromeo, U. Zimmermann, S. Andò, G. Coletti, D. Bersani, D. Basso, P. Gentile, B. Schulz, E. Garzanti, Raman spectroscopy as a tool for magnesium estimation in Mg-calcite, *J. Raman Spectrosc.* 2017, **48**, 983-992.